Title

Instantaneous movement-unrelated midbrain activity modifies ongoing eye movements

Authors

Antimo Buonocore[1,2], Matthias P. Baumann[1,2], Ziad M. Hafed[1,2]

1. Werner Reichardt Centre for Integrative Neuroscience, Tübingen University, Tübingen, BW, 72076, Germany
2. Hertie Institute for Clinical Brain Research, Tübingen University, Tübingen, BW, 72076, Germany

Corresponding author:

Antimo Buonocore
Werner Reichardt Centre for Integrative Neuroscience
Otfried-Müller Str. 25
Tübingen, 72076, Germany
Tel: +49 7071 29 88821
antimo.buonocore@cin.uni-tuebingen.de

Abstract

At any moment in time, new information is sampled from the environment and interacts with ongoing brain state. Often, such interaction takes place within individual circuits that are capable of both mediating the internally ongoing plan as well as representing exogenous sensory events. Here we investigated how sensory-driven neural activity can be integrated, very often in the same neuron types, into ongoing oculomotor commands for saccades. Despite the ballistic nature of saccades, visually-induced action potentials in the superior colliculus (SC), a structure known to drive eye movements, not only occurred intra-saccadically, but they were also associated with highly predictable modifications of the ongoing eye movements. Such modifications were also possible by peri-saccadically injecting single, double, or triple electrical microstimulation pulses into the SC. Our results suggest instantaneous readout of the SC map during movement generation, irrespective of activity source, and explain a significant component of kinematic variability of motor outputs.

Introduction

A hallmark of the central nervous system is its ability to process an incredibly complex amount of incoming information from the environment in parallel. This is achieved through multiplexing of functions, either at the level of individual brain areas or even at the level of individual neurons themselves. For example, in different motor modalities like arm (Alexander and Crutcher, 1990; Shen and Alexander, 1997; Breveglieri et al., 2016) or eye (Goldberg and Wurtz, 1972b, a; Wurtz and Goldberg, 1972; Mohler and Wurtz, 1976; Bruce and Goldberg, 1985) movements, a large fraction of the neurons contributing to the motor command are also intrinsically sensory in nature, hence being described as sensory-motor neurons. In this study, we aimed to investigate the implications of such sensory and motor multiplexing using vision and the oculomotor system as our model of choice.

A number of brain areas implicated in eye movement control, such as the midbrain superior colliculus (SC) (Wurtz and Albano, 1980; Munoz and Wurtz, 1995), frontal eye fields (FEF) (Bruce and Goldberg, 1985; Schall and Hanes, 1993; Schall et al., 1995; Tehovnik et al., 2000), and lateral intra-parietal area (LIP) (Mazzoni et al., 1996), contain many so-called visual-motor neurons. These neurons burst both in reaction to visual stimuli entering into their response fields (RF's) as well as in association with triggering eye movements towards these RF's. In some neurons, for example in the SC (Mohler and Wurtz, 1976; Mays and Sparks, 1980; Edelman and Goldberg, 2001; Willeke et al., 2019), even the motor bursts themselves are contingent on the presence of a visual target at the movement endpoint. In the laboratory, the properties of visual and motor bursts are frequently studied in isolation, by dissociating the time of visual onsets (evoking "visual" bursts) from the time of saccade triggering (evoking "motor" bursts). However, in real life, exogenous sensory events can happen at any time in relation to our own ongoing internal state. Thus, "visual" spikes at one visual field location may, in principle, be present at the same time as "motor" spikes for a saccade to another location. What are the implications of such simultaneity? Answering this

question is important to clarify mechanisms of readout from circuits in which functional multiplexing is prevalent.

In the SC, our focus here, there have been many debates about how this structure contributes to saccade control (Waitzman et al., 1991; Ivan et al., 2018). In recent proposals (Goossens and Van Opstal, 2006; Van Opstal and Goossens, 2008; Goossens and Van Opstal, 2012), it was suggested that every spike emitted by SC neurons during their “motor” bursts contributes a mini-vector of movement tendency, such that the aggregate sum of all output spikes is read out by downstream structures to result in a given movement trajectory. However, implicit in these models is the assumption that only action potentials within a narrow time window around movement triggering (the “motor” burst) matter. Any other spiking, by the same or other neurons, before or after the eye movement is irrelevant. This causes a significant readout problem, since downstream neurons do not necessarily have the privilege of knowing which spikes should now count for a given eye movement implementation and which not.

Indeed, from an ecological perspective, an important reason for multiplexing could be exactly to maintain flexibility to rapidly react to the outside world, even in a late motor control structure. In that sense, rather than invoking mechanisms that allow actively ignoring “other spiking” activity outside of the currently triggered eye movement (whether spatially or temporally), one would predict that SC readout, at any one moment, should be quite sensitive to any spiking activity regardless of its source. We experimentally tested this hypothesis. We “injected” SC spiking activity around the time of saccade generation, but at a spatially dissociated location. We uncovered causal evidence that the entire landscape of SC activity can instantaneously contribute to individual saccade metrics, explaining a component of behavioral variability previously unaccounted for.

Results

Stimulus-driven SC "visual" bursts can occur intra-saccadically

We first tested the hypothesis that visually-induced action potentials can occur in the SC intra-saccadically; that is, simultaneously with motor-related bursts. We exploited the topographic nature of the SC in representing visual and motor space (Cynader and Berman, 1972; Robinson, 1972; Chen et al., 2019). We asked two monkeys (P and N) to maintain steady fixation on a central spot. Prior work has shown that this condition gives rise to frequent microsaccades, which are associated with movement-related bursts in the rostral region of the SC representing small visual eccentricities and movement vectors (Hafed et al., 2009; Hafed and Krauzlis, 2012a; Chen et al., 2019; Willeke et al., 2019). We then presented a visual stimulus at a more eccentric location, and we recorded neural activity at this location (Fig. 1A, B). Depending on the timing of the visual stimulus relative to a given microsaccade, we could measure visual burst strength (in both visual and visual-motor neurons; Methods) either in isolation of microsaccades or when a microsaccade was in-flight. If SC visual bursts could still occur intra-saccadically, then one would expect that visual burst strength should be similar whether the burst timing happened when a microsaccade was being triggered or not. We ensured that all sites did not simultaneously burst for microsaccade generation (Figs. 1B, S1), to ensure that we were only measuring visual bursts and not concurrent movement-related activity. Such movement-related activity was expectedly in more rostral SC sites, representing foveal visual eccentricities, as we also confirmed in the same two monkeys (and sometimes in the very same sessions) in an earlier report (Chen et al., 2019).

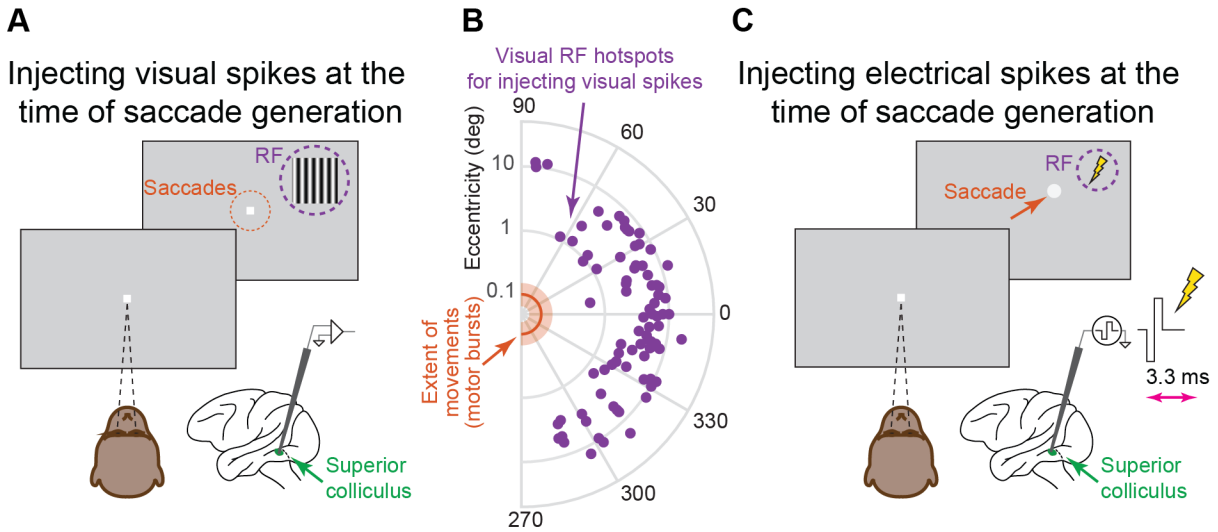

Figure 1 Injecting arbitrary, movement-unrelated spiking activity into the SC map around the time of saccade generation. (A) A monkey steadily fixated while we presented an eccentric stimulus in a recorded neuron's RF (purple). The stimulus location was spatially dissociated from the motor range of microsaccades being generated (orange circles). This allowed us to experimentally inject movement-unrelated "visual" spikes into the SC map around the time of microsaccade generation. **(B)** We injected "visual" spikes at eccentric retinotopic locations (purple dots) distinct from the neurons that would normally exhibit motor bursts for microsaccades. The orange line and shaded area denote the mean and 95% confidence interval, respectively, of all microsaccade amplitudes that we observed. The neurons in which we injected "visual" spikes (purple dots) were not involved in generating these microsaccades (Fig. S1). The origin of the shown log-polar plot corresponds to 0.03 deg eccentricity (Hafed and Krauzlis, 2012b). **(C)** In a second experiment, a monkey generated a saccade to a given target location. We injected single, double, or triple "electrical" spikes into the SC map, again at a site unrelated to the currently generated saccade (purple RF and yellow symbol for the microstimulated site, versus orange for the saccade vector). The relative relationship between saccade target eccentricity and microstimulated SC site was similar to the relative relationship between movement sizes and "visual" spikes in **A**: in both cases, we injected movement-unrelated SC activity at a site more eccentric than the internally generated movement.

Regardless of microsaccade direction, "visual" bursts could still occur in the SC even if there was an ongoing eye movement. To illustrate this, Fig. 2A shows the stimulus-driven visual burst of an example neuron with and without concurrent microsaccades. The stimulus in this case consisted of a vertical sine wave grating of 40% or 80% contrast (Methods). The top panel of the figure shows the times of microsaccade onsets (crosses) and ends (squares) for all movements occurring in the session that overlapped with the interval of visual burst occurrence, which we defined to be 30-100 ms. This latter interval was chosen based on the bottom panel of the figure, showing the actual visual bursts. The gray curve shows average firing rate when there were no microsaccades from -100 ms to +150 ms relative to stimulus onset, and the orange curve shows average firing rate when the visual burst (shaded interval) coincided with at least a part of an ongoing microsaccade (top panel).

As can be seen, intra-saccadic “visual” bursts could still occur, and they were similar in strength to saccade-free visual bursts. This was true across our population; for each neuron, we plotted in Fig. 2B peak firing rate after stimulus onset when there was a concurrent microsaccade being generated (inset schematic near the y-axis) as a function of peak firing rate after stimulus onset when there was no concurrent microsaccade (inset schematic near the x-axis). For this analysis, we pooled trials from the highest 3 contrasts (20%, 40%, and 80%) that we used in our study for simplicity (Methods), but similar conclusions could also be reached for individual stimulus contrasts. There was no difference in visual burst strength as a function of coincident microsaccades ($t(84) = 1.6905$, $p = 0.09$). Moreover, SC visual bursts could still occur intra-saccadically whether the stimulus was activating the same SC side generating a given movement or the opposite SC side (Fig. S2).

Therefore, at the time of movement execution (that is, at the time of a movement-related burst in one part of the SC map), it is possible to have spatially dissociated visual bursts in another part of the map. We next investigated how such additional “visual” spikes (at an unrelated spatial location relative to the movements) affected the eye movements that they were coincident with.

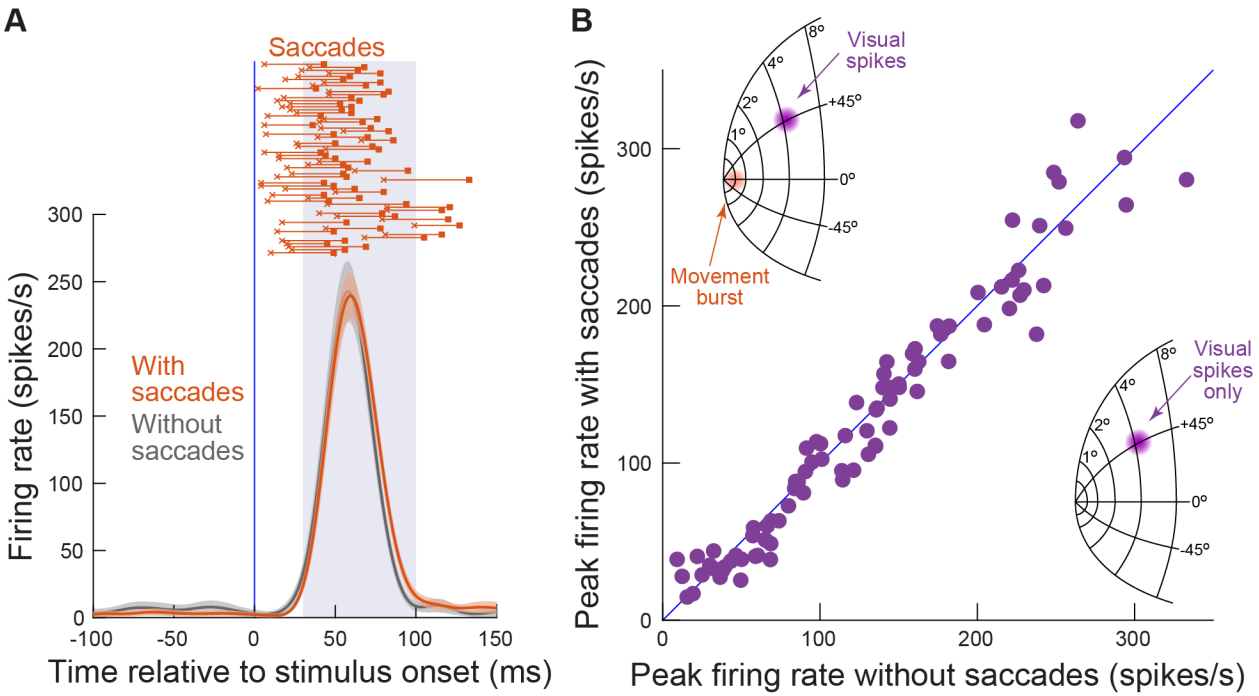

Figure 2 SC visual bursts can still occur intra-saccadically. **(A)** We measured the firing rate of an example neuron when a stimulus appeared inside its RF without any nearby microsaccades (gray firing rate curve) or when the same stimulus appeared while microsaccades were being executed around the time of visual burst occurrence (orange firing rate curve). The raster above the firing rate curves shows the individual microsaccades that occurred in the session for the orange firing rate curve (cross means movement onset, and square means movement end). For all of the movements, the visual burst overlapped with at least parts of the movements. Error bars denote 95% confidence intervals, and the shaded violet region denotes our estimate of visual burst interval (30-100 ms after stimulus onset). **(B)** At the population level, there was no difference in peak firing rate with saccades detected during a visual burst (y-axis and schematic near it) or without saccades around the visual burst (x-axis and schematic near it). The y-axis data correspond to the top left schematic view of the SC map (Hafed and Chen, 2016), in which extra-foveal visual spikes (purple) occurred in the SC concurrently with foveal motor spikes (orange) triggering microsaccades. The x-axis data correspond to the situation in the bottom right schematic, with no movement-related motor bursts at the time of the visually-induced spikes.

Peri-saccadic stimulus-driven "visual" bursts systematically influence eye movement metrics

If "visual" bursts can be present somewhere on the SC map at a time when "motor" bursts elsewhere on the map are to be read out by downstream neurons, then one might expect that each additional "visual" spike on the map should contribute to the executed movement metrics and cause a change in saccades. This would suggest a highly lawful relationship between the strength of the peri-saccadic "visual" burst and the amount of eye movement alteration that is observed. We explored this by relating the behavioral properties of the saccades in our task to the temporal relationship between their onset and the presence of "visual" spikes in the SC map caused by an unrelated stimulus onset.

We first confirmed a clear correlation between microsaccade amplitudes and eccentric stimulus onsets (Hafed and Ignashchenkova, 2013; Buonocore et al., 2017b; Malevich et al., 2020a). Our stimuli consisted of vertical sine wave gratings having different luminance contrasts (Methods). We plotted the time course of microsaccade amplitudes relative to grating onset for microsaccades that were spatially congruent with grating location (that is, having directions towards grating location; Methods). For the present analysis, we only focused on stimulus eccentricities of ≤4.5 deg because these had the strongest effects on microsaccades (Fig. S3). As expected (Hafed and Ignashchenkova, 2013; Buonocore et al., 2017b; Malevich et al., 2020a), there was a transient increase in microsaccade amplitude approximately 80-90 ms after grating onset (Fig. 3A). Critically, the increase reflected the stimulus properties, because it was stronger with higher stimulus contrast (main effect of contrast: $F(2,713) = 81.55$, $p < 1.27427*10^{-32}$), and there were also qualitatively different temporal dynamics: amplitude increases occurred earlier for higher (~75 ms) than lower (~85 ms) contrasts. Because we had simultaneously recorded neural data, we then analyzed, for the same trials, the SC visual bursts that were associated with the appearing gratings in these sessions. Visual bursts started earlier, and were stronger, for higher stimulus contrasts (Fig. 3B) (Li and Basso, 2008; Chen et al., 2015), similar to the amplitude changes in microsaccades. Moreover, the timing of the microsaccadic effects (Fig. 3A) was similar to the timing of the SC visual bursts (Fig. 3B), showing a short lag of ~20 ms relative to the bursts that is consistent with an efferent processing delay from SC neurons to the final extraocular muscle drive.

Therefore, as we hypothesized in previous reports (Hafed and Ignashchenkova, 2013; Buonocore et al., 2017b; Malevich et al., 2020a), not only is it possible for SC visual bursts to occur intra-saccadically (Fig. 2), but such bursts are temporally aligned with concurrent changes in microsaccade amplitudes (Fig. 3). We next uncovered a highly lawful impact of each injected extra “spike” per recorded neuron on saccade metrics.

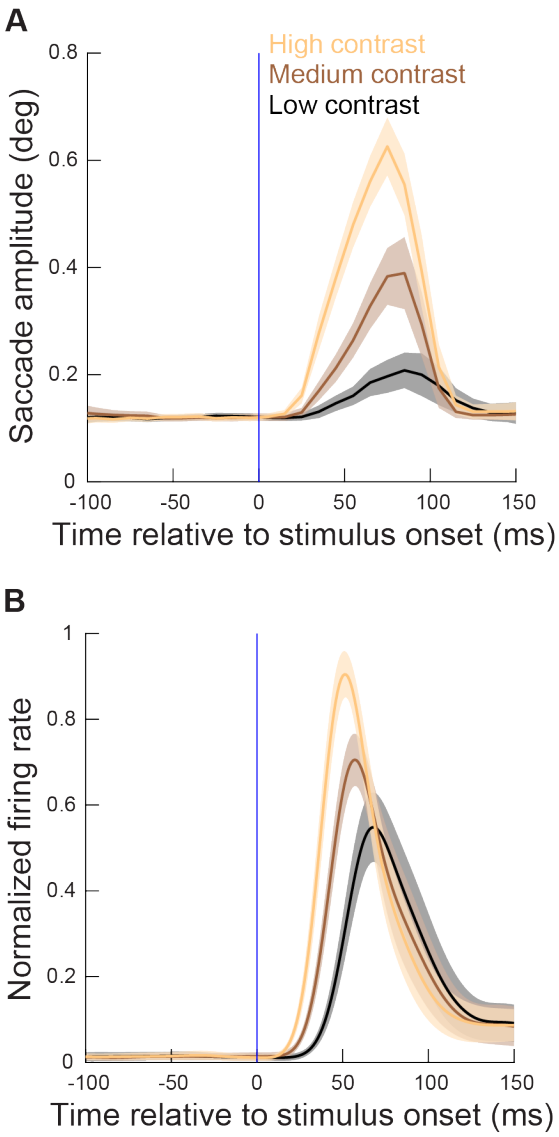

Figure 3 Saccade metrics are altered when the movements coincide with SC visual bursts, and the alteration is related to SC visual burst strength. (A) Time course of saccade amplitude in our task relative to stimulus onset (vertical blue line). The data were subdivided according to stimulus contrast (three different colors representing the three highest contrasts in our task). Movements amplitudes were small (microsaccades) in the baseline pre-stimulus interval, but they sharply increased after stimulus onset, reaching a peak at around 70-80 ms. Moreover, the metric alteration clearly depended on stimulus contrast. **(B)** Normalized firing rates relative to stimulus onset (vertical blue line) for all extra-foveal neurons that we recorded simultaneously with the eye movement data in **A**. The alterations in movement metrics in **A** were strongly correlated in both time and amplitude with the properties of SC visual bursts. Error bars denote 95% confidence intervals. Figs. S3, S4 shows results with more eccentric neurons and stimuli (>4.5 deg).

The number of extra “visual” spikes per recorded neuron occurring intra-saccadically was linearly related to metric alterations in microsaccades. For each eye movement towards the recently appearing stimulus (that is, congruent with stimulus location), we counted how many “visual” spikes by the concurrently recorded neuron occurred in the interval between eye movement onset and saccade peak velocity. That is, we tested for the impact of the

number of extra “visual” spikes by a given recorded neuron as the SC population was being read out by downstream pre-motor and motor structures to execute the triggered movement. This per-neuron spike count was a proxy for how adding additional “visual” spikes in the SC population at a site unrelated to the movement vector can “leak” downstream when the saccade gate is opened. Moreover, since the extra spikes were more eccentric than the sizes of the congruent microsaccades, we expected that the contribution would act to increase microsaccade amplitudes (as in Fig. 3A). We focused, for now, on neurons at eccentricities ≤4.5 deg (but still more eccentric than microsaccade amplitude; Fig. 1B) because our earlier analyses showed that the clearest metric changes to tiny microsaccades occurred under these circumstances (Figs. 3, S3, S4). We found a clear, lawful relationship between the amount of “extra” spikes that occurred intra-saccadically on movement metrics. These spikes were unrelated to the originally planned “motor” burst; they were spatially dissociated but temporally coincident with saccade triggering, and they were also driven by an exogenous visual stimulus onset. To demonstrate this observation, we plotted in Fig. 4A the average microsaccadic eye movement trajectory in the absence of any additional SC “visual” bursts (dark red; the curve labeled 0 spikes; Methods). We then plotted average microsaccade size whenever any given recorded eccentric neuron had a visual burst such that 1 spike of this visual burst happened to occur between movement onset and movement peak velocity (red; 1 spike). The amplitude of the microsaccade was significantly larger than with 0 spikes. We then progressively looked for movements with 2, 3, 4, 5, or 6 “visual” spikes per recorded neuron that happened to occur intra-saccadically; there were progressively larger and larger microsaccades (Fig. 4A). Across all data, the number of “visual” spikes (per recorded neuron) that occurred intra-saccadically was lawfully and linearly driving the amplitude increase of the (smaller) saccades (Fig. 4B) (Towards condition, F-statistic vs. constant model: $F = 799$, $p<0.0001$; estimated coefficients : intercept = 0.1412, $t = 30.0298$, $p<0.0001$; slope = 0.0914, $t = 28.26$, $p<0.0001$). On the

other hand, microsaccades directed opposite to the RF did not show any systematic modulation by the number of injected intra-saccadic spikes (Opposite condition, F-statistic vs. constant model: $F = 3.83$, $p = 0.05$; estimated coefficients: intercept = 0.11553, t = 57.13.0298, $p<0.0001$; slope = 0.0048, t = 1.9584, $p = 0.05$), suggesting that it is difficult to reduce microsaccade size below the already small amplitude of these tiny eye movements (Hafed, 2011).

These results suggest that there is an instantaneous specification of saccade metrics described by the overall activity present on the SC map, and they provide a much more nuanced view of the correlations between SC visual bursts and microsaccade amplitudes shown in Fig. 3. Every SC spike matters: all activity happening intra-saccadically and at locations of the SC map different from the saccade endpoint goal is interpreted as part of the motor command by downstream neurons.

For completeness, we also considered the same analyses as in Fig. 4 (that is, with congruent movements) but for more eccentric SC “visual” bursts (Fig. S5). The effects were present but in a significantly weaker manner than in Fig. 4, suggesting that the distance of the “extra” spiking activity on the SC map from the planned movement vector matters (Towards condition, F-statistic vs. constant model: $F = 77.1$, $p<2.13*10^{-18}$; estimated coefficients : intercept = 0.12254, t = 60.889, $p<0.0001$; slope = 0.012496, t = 8.7813, $p<2.13*10^{-18}$). This observation, while still showing that every spike matters, is inconsistent with recent models of saccade generation by the SC (Goossens and Van Opstal, 2006; Van Opstal and Goossens, 2008; Goossens and Van Opstal, 2012), which do not necessarily implement any kind of local versus remote interactions in how the SC influences saccade trajectories through individual spike effects.

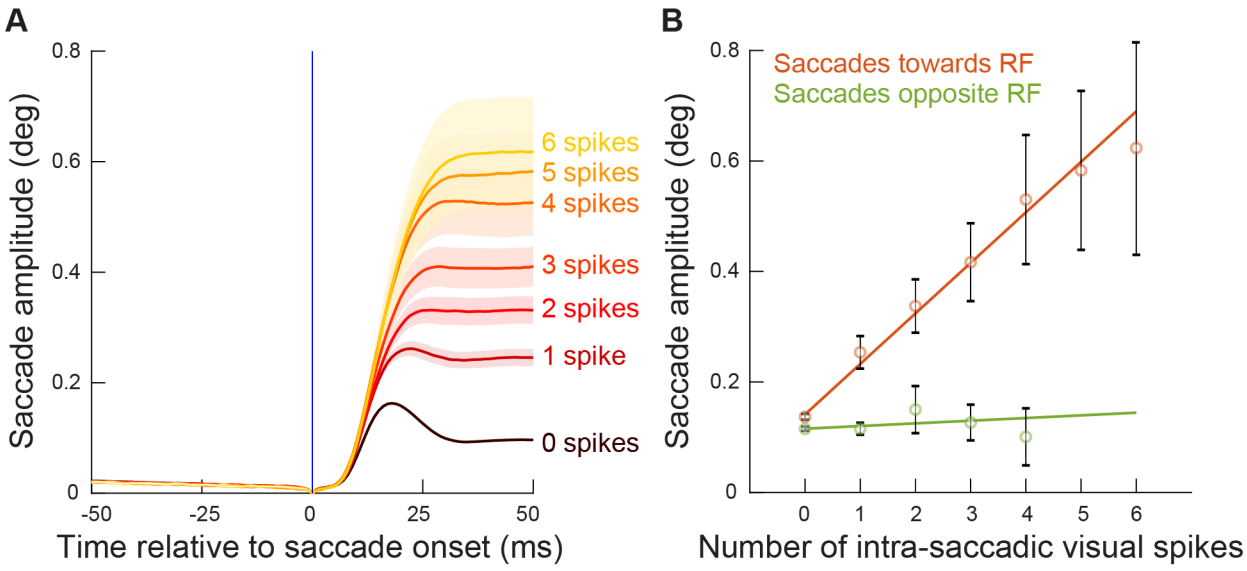

Figure 4 The number of exogenous, movement-unrelated "visual" spikes to occur intra-saccadically linearly adds to the executed movement's amplitude. (A) For every recorded neuron from Fig. 3 and every microsaccade to occur near the visual burst interval (Fig. 1), we counted the number of spikes recorded from the neuron that occurred intra-saccadically (between movement onset and movement peak velocity). We did this for movements directed towards the RF location (Fig. 1B; Methods). We then plotted radial eye position (aligned to zero in both the x- and y-axes) relative to saccade onset after categorizing the movements by the number of intra-saccadic spikes. When no spikes were recorded during the eye movement, saccade amplitudes were small (darkest curve), consistent with microsaccades during steady fixation. Adding "visual" spikes in the SC map during the ongoing movement systematically increased movement amplitudes. Error bars denote s.e.m. **(B)** To summarize the results in **A**, we plotted mean saccade amplitude against the number of intra-saccadic "visual" spikes for movements directed towards the RF locations (faint red dots). There was a linear increase in amplitude with each additional spike per recorded neuron (orange line representing the best linear fit of the underlying raw data). For movements opposite the RF locations (faint green dots and green line), there was no impact of intra-saccadic "visual" spikes on movement amplitudes. Error bars denote one standard error of the mean (**A**) and (**B**) 95% confidence intervals. Fig. S5 shows results for intra-saccadic spikes from more eccentric neurons (>4.5 deg).

To further investigate the results of Fig. 4, we next explored more detailed temporal interactions between SC visual bursts and saccade metric changes. Across all trials from all neurons analyzed in Fig. 4, we measured the time of any given trial's visual burst peak relative to either microsaccade onset (Fig. 5A), microsaccade peak velocity (Fig. 5B), or microsaccade end (Fig. 5C), and we sorted the trials based on burst peak time relative to microsaccade onset (i.e. the trial sorting in all panels in Fig. 5 was always based on the data from panel A). We then plotted individual trial spike rasters with the bottom set of rasters representing trials with the SC "visual" burst happening much earlier than microsaccade onset and the top set being trials with the SC "visual" burst occurring after microsaccade end. The rasters were plotted in gray in Fig. 5, except that during a putative visual burst

interval (30-100 ms from stimulus onset), we color-coded the rasters by the microsaccade amplitude observed in the same trials (same color coding scheme as in Fig. 4A). The marginal plot in Fig. 5D shows microsaccade amplitudes for the sorted trials (with a moving average window of 30 trials in steps of 30 trials; Methods). We used this marginal plot to estimate which sorted trials were associated with the beginning of microsaccade amplitude increases (from the bottom of the raster and moving upward) and which trials were associated with the end of the microsaccade amplitude increases. As can be seen, whenever SC “visual” bursts occurred pre- and intra-saccadically, microsaccade amplitudes were dramatically increased by two- to three-fold relative to baseline microsaccade amplitudes (blue horizontal lines). For visual bursts after peak velocity (Fig. 5C), the effect was diminished, consistent with efferent delays from SC activity to extraocular muscle activation (Miyashita and Hikosaka, 1996; Munoz et al., 1996; Stanford et al., 1996; Gandhi and Keller, 1999a; Katnani and Gandhi, 2012).

Therefore, at the time in which SC activity is to be read out by downstream neurons to implement a saccadic eye movement (right before movement onset to right before movement end, e.g. Miyashita and Hikosaka, 1996; Munoz et al., 1996; Stanford et al., 1996; Gandhi and Keller, 1999a; Katnani and Gandhi, 2012), additional movement-unrelated SC spiking activity is also read out and has a direct impact on eye movement metrics.

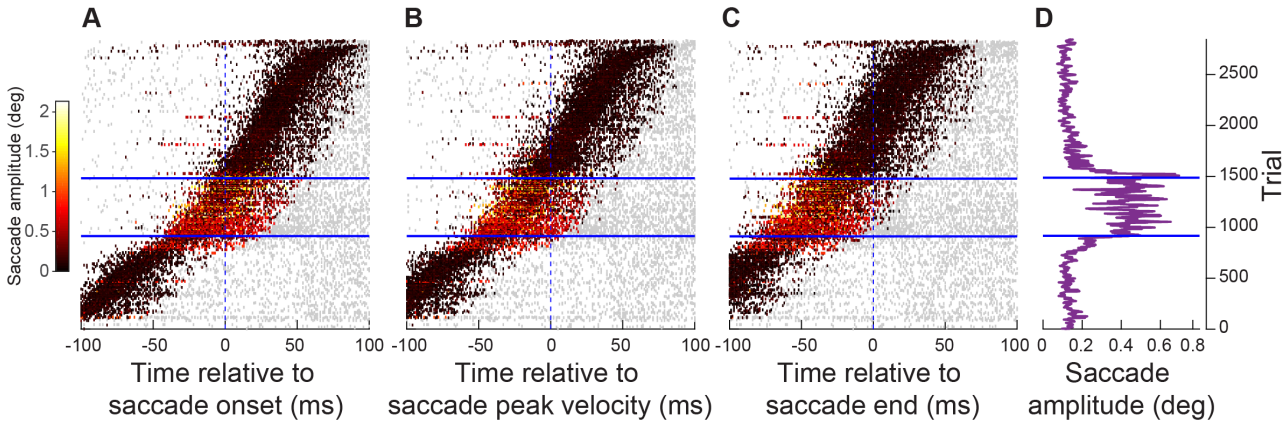

Figure 5 Exogenous, movement-unrelated SC spikes have the greatest impact on movement metrics when they occur peri-saccadically. (A) Individual trial spike rasters across all neurons ≤4.5 deg eccentricity and all movements towards RF locations. The spike rasters are sorted based on the time of the visual burst (peak firing rate after stimulus onset) relative to saccade onset (bottom left: trials with visual bursts earlier than microsaccades; top right: trials with visual bursts later than microsaccades). The spike rasters are plotted in gray except during the interval 30-100 ms after stimulus onset (our visual burst interval; Fig. 2) to highlight the relative timing of the visual burst to movement onset. Spikes in the visual burst interval are color-coded according to the observed movement amplitude on a given trial (legend on the left). As can be seen, microsaccades were enlarged when extra-foveal SC spiking (stimulus-driven visual bursts) occurred right before and during the microsaccades (see marginal plot of movement amplitudes in **D**). **(B)** Same as **A**, and with the same trial sorting, but with burst timing now aligned to movement peak velocity. **(C)** Same as **A**, **B**, and with the same trial sorting, but with burst timing now aligned to movement end. The biggest amplitude effects occurred when the exogenous "visual" spikes occurred pre- and intra-saccadically, but not post-saccadically. **(D)** Microsaccade amplitudes (30-trial moving average) on all sorted trials in **A**-**C**. Blue horizontal lines denote the range of trials for which there was a significant increase in movement amplitudes (Methods).

To obtain even more precise knowledge of the time needed for any injected "visual" spikes to start influencing saccade metrics, we then selected all individual trial spike rasters from Fig. 5A, and we counted the number of spikes occurring within any given 5 ms time bin relative to eye movement onset. We did this for all time bins between -100 ms and +100 ms from movement onset, and we also binned the movements by their amplitude ranges (Fig. 6A). The two smallest microsaccade amplitude bins reflected baseline movement amplitudes (see Fig. 3A), and they expectedly occurred when there was no "extra" spiking activity in the SC around their onset (Fig. 6A, two darkest reds). For all other amplitude bins, the larger movements were always associated with the presence of extra "visual" spikes on the SC map (more eccentric than the normal microsaccade amplitudes) occurring between -30 ms and +30 ms from saccade onset (Fig. 6A). Note how the timing of the effect was constant across amplitude bins, suggesting that it is the relative timing of extra "visual"

spikes and movement onset that mattered; the amplitude effect (that is, the different colored curves) simply reflected the total number of spikes that occurred during the critical time window of movement triggering (consistent with Fig. 4). Therefore, additional “visual” spikes in the SC at a time consistent with saccade-related readout by downstream neurons essentially “leak” into the saccade being generated. On the other hand, the pattern of Fig. 6A was not present for movements going opposite to the recorded neuron’s RF’s, for which, if anything, there was a lower number of spikes happening during the peri-saccadic interval (Fig. 6B). This suggests that it was easier to trigger microsaccades in one direction when no activity was present in the opposite SC.

The strongest evidence that any “extra” spiking activity present on the SC map can systematically alter the amplitude of the eye movements, irrespective of our experimental manipulation of visual bursts, can be seen in Fig 6C. Here, we selected microsaccades launched 100 ms after grating onset, temporally distant from the time of the earlier visual bursts. This was to demonstrate that there is actually no need for a stimulus-driven visual burst to be present for us to observe effects of extraneous spiking activity on triggered eye movements. We counted the number of spikes occurring within the first 25 ms of the selected movements. Because sustained firing rates were relatively low, which reduced the total amount of data available to us for this analysis, we restricted the analysis to microsaccades in which we could count either 2, 3, or 4 “extra” spikes emitted by a given recorded neuron during the microsaccades. Even when the spikes were no longer strongly associated with the stimulus-induced visual burst, their presence on the SC map at a site more eccentric than microsaccade amplitudes was enough to modulate eye movement amplitudes in a systematic manner, increasing the amplitude above baseline levels (blue line) when more spikes were present. Such modulation was again not visible for movements going in the opposite direction from the recorded neuron’s RF’s (Fig. 6D), again suggesting

that there is a lower limit to how small microsaccades can become with opposite drive from the other SC.

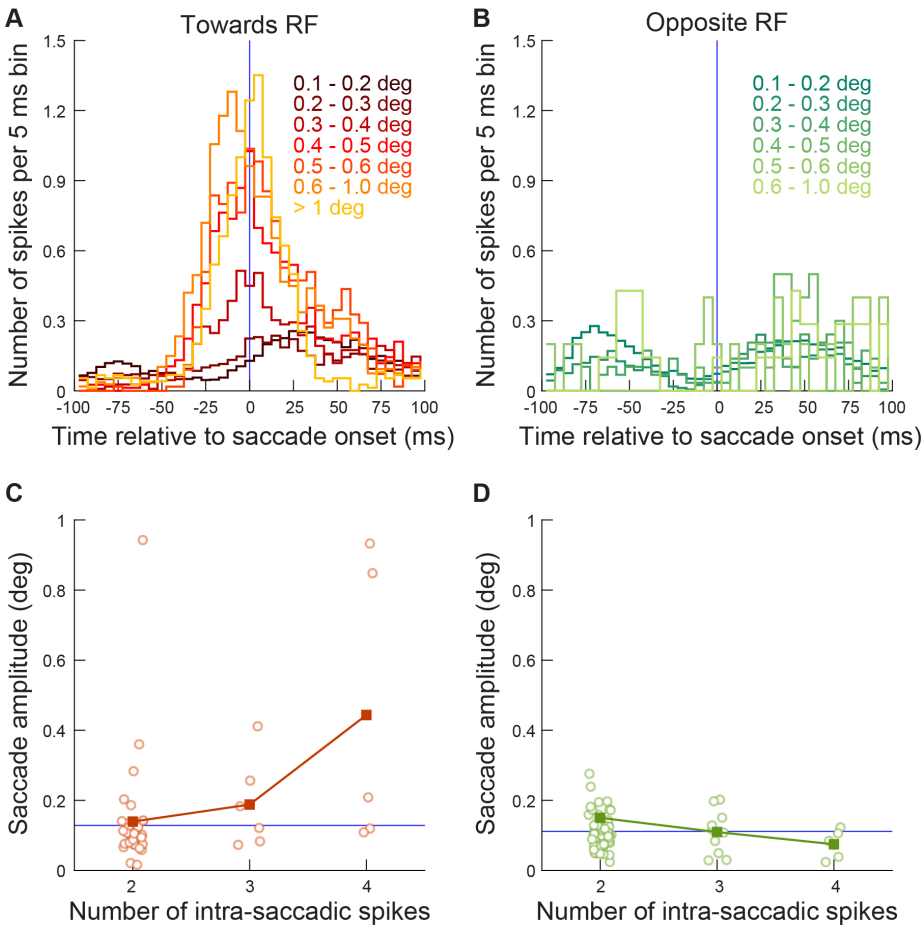

Figure 6 Exogenous, movement-unrelated "visual" spikes affect movement metrics when they occur within approximately +/- 30 ms from movement onset, and they need not be part of a stimulus-driven visual burst to be effective. (A) For different microsaccade amplitude ranges from Fig. 5 (color-coded curves), we counted the number of exogenous spikes occurring from a recorded extra-foveal SC neuron within any given 5 ms time bin around movement onset (range of times tested: -100 ms to +100 ms from movement onset). The lowest two microsaccade amplitude ranges (0.1-0.2 and 0.2-0.3 deg) reflected baseline amplitudes during steady-state fixation (e.g. Fig. 3), and they were not correlated with additional extra-foveal spiking activity around their onset (two darkest red curves). For all other larger microsaccades, they were clearly associated with precise timing of extra-foveal "visual" spikes occurring within approximately +/- 30 ms from movement onset, regardless of movement size. **(B)** Same as **A** but for movements opposite the recorded neuron's RF locations. There were fewer spikes during the peri-saccadic interval, suggesting that it was easier to trigger eye movements when there was no activity present in the opposite SC. **(C)** Relation between the number of intra-saccadic spikes and saccade amplitudes for eye movements triggered 100 ms after grating onset, temporally distant from the time of the visual burst. Each dot represents a saccade amplitude with the associated number of spikes detected within 25 ms after movement onset. Solid squares represent the averages. The presence of intra-saccadic spikes on the SC map was enough to modulate movement amplitudes even outside of our usual visual burst interval of earlier analyses. Blue indicates baseline microsaccade amplitude. **(D)** Same as **C** but for movements opposite the recorded RF location.

Overall, these results demonstrate that there is a tight time window around saccade onset (Fig. 6) in which any movement-unrelated spikes in sites other than the saccade goal representation can induce a systematic variation in the motor program.

Peri-saccadic single, double, or triple pulse electrical microstimulation alters eye movement metrics

Our results so far demonstrate that as little as one single extra action potential by each visually-activated neuron was sufficient to alter ongoing microsaccades (Figs. 4-6). To establish a causal role for such exogenous SC spiking activity, we next replaced visual stimulus onsets with single, double, or triple electrical microstimulation pulses that were strategically timed to occur peri-saccadically. We did this in a third monkey (M) for which we know that amplitude effects like those in Fig. 3 still took place (Buonocore et al., 2019; Malevich et al., 2020a). We performed an experiment analogous to peri-saccadic perceptual experiments in which brief visual stimuli occur near the time of saccade onset (e.g. Honda, 1989; Morrone et al., 1997; Ross et al., 1997; Lappe et al., 2000; Krekelberg et al., 2003; Buonocore et al., 2017a; Grujic et al., 2018), but we replaced visual stimuli with “electrical” stimuli. The monkey generated an instructed visually-guided saccade, and we introduced electrical microstimulation pulses at random times (Methods). To simulate the effects of Figs. 4-6 in this “electrical” spiking paradigm, we had the monkey generate visually-guided saccades to a parafoveal location (2.2–5.5 deg across sessions), and the microstimulating electrode was always at a site representing a larger eye movement vector along the same direction (Methods). This makes the experiment similar in principle to the conditions of Figs. 4-6 above: additional spiking activity in the same SC but at a location more eccentric than that of the planned eye movement. Prior to microstimulation, we confirmed that the visually-guided saccade target location was outside of the visual and movement RF’s at the microstimulated SC site. That is, the microstimulated SC site was not directly involved in

generating the visually-guided saccade; it was just injecting extraneous spikes analogous to the “visual” spikes in Figs. 2-6. More importantly, we confirmed that triple pulse microstimulation, the strongest of our electrical manipulations, did not itself evoke any systematic saccadic eye movements (even microsaccades) during a control fixation condition (Fig. S6). We then proceeded to the main experiment.

Figure 7 shows results from an example microstimulation session. In Fig. 7A, we plotted the trajectories of saccades to a location approximately 1.9 deg to the right and 3 deg above fixation without coincident microstimulation. In Fig. 7B (red traces), the monkey generated the same visually-guided saccades, but these saccades were now paired with 3 microstimulation pulses (inter-pulse interval: 3.3 ms; 30 μA current amplitude per pulse; Methods) starting within +/-10 ms of movement onset. The saccades were now elongated relative to the baseline saccades (also shown in faint color in Fig. 7B to facilitate comparison between the two conditions), consistent with the results of Figs. 4-6 above. Thus, the saccades were pulled towards the site in which additional SC spiking was injected, such that the overall displacement of the eye during the saccades was slightly longer. Such elongation was further clarified when we plotted radial eye velocity. Injecting 3 microstimulation pulses at saccade onset introduced a secondary velocity transient, shortly afterwards, to elongate the movements relative to baseline (Fig. 7C, D). Therefore, exogenous movement-unrelated “electrical” activity had a similar effect to the “visual” activity described in our earlier experiments.

Across sessions, we tested single, double, or triple pulse microstimulation in peri-saccadic intervals. To summarize all results, we first defined a baseline saccadic displacement amplitude as the overall displacement caused by saccades in which no microstimulation pulse occurred near saccade onset (Methods). We then obtained a time course of saccadic displacement as a function of peri-saccadic microstimulation pulses by measuring, for any time window of pulse times relative to saccade onset, the saccadic

displacement observed and normalizing it to the baseline displacement. This gave us a percentage change of saccadic displacements as a function of microstimulation pulse times relative to saccade onset, and it also allowed us to summarize all sessions together when they individually each had slightly different SC sites being microstimulated. As shown in Fig. 8, even single and double pulse microstimulation affected ongoing eye movement metrics. The increase in eye displacement started about 25 ms before saccade onset, and it lasted for 25 ms thereafter, consistent with the timing described in Fig. 6. Moreover, consistent with Figs. 4-6, the amplitude changes were sensitive to the number of injected microstimulation pulses. With one injected “electrical” spike, the alteration in the displacement was modest (~6%) and loosely centered around the saccade onset. With two and three injected spikes, the alteration was significantly stronger (~8%) and in a more precise time window around the saccade. Overall, the trajectories were clearly pulled towards the RF locations of the stimulated sites.

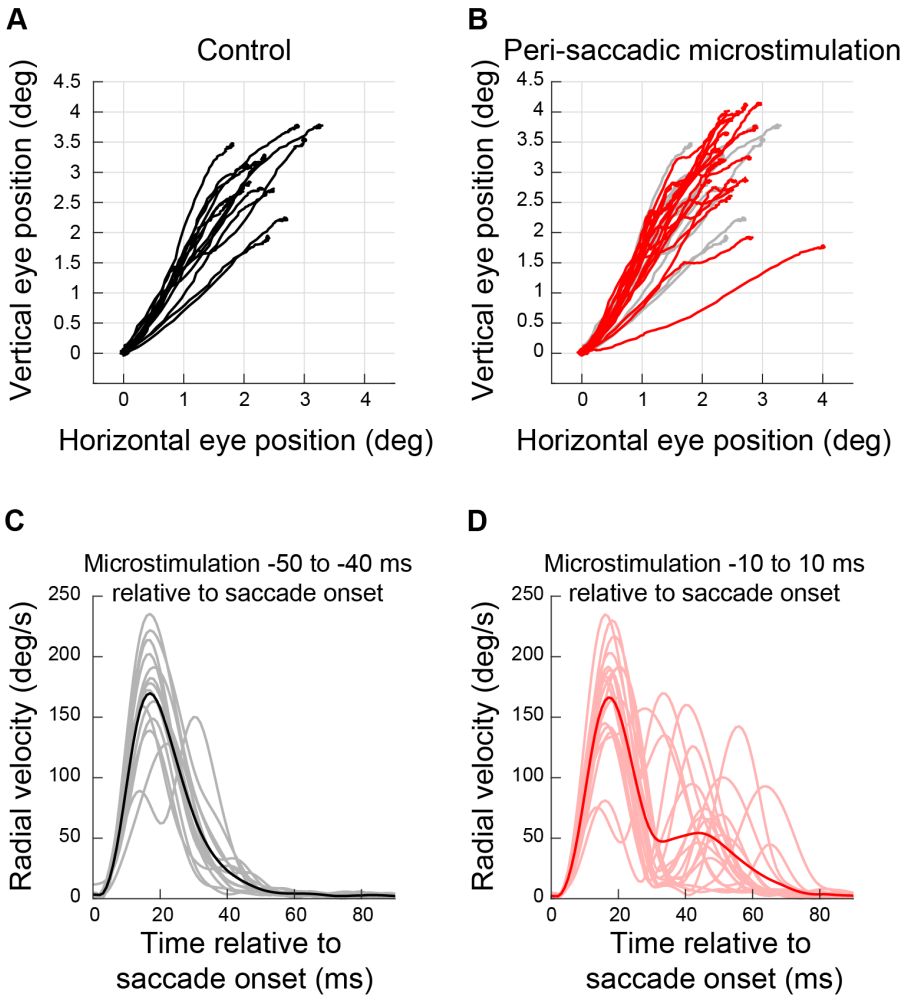

Figure 7 Replacing "visual" with "electrical" exogenous spikes similarly alters ongoing eye movement metrics. Example session from the experiment of Fig. 1C. A monkey generated a saccade to a target at 1.9 deg and 3 deg horizontally and vertically, respectively. In a control manipulation (**A**), 3 pulses of electrical microstimulation were injected into the SC 40-50 ms before saccade onset, and at a site more eccentric than the saccade target (but along a similar vector direction; Methods). In peri-saccadic microstimulation (**B**), the same 3 pulses were applied to the same SC site, but now within +/- 10 ms from saccade onset. Each curve in **A**, **B** shows the total saccadic displacement of the eye on individual trials (from 50 ms before saccade onset to 100 ms afterwards), and the curves were all aligned together at the origin (eye position at saccade onset). The gray curves in **B** are the same as those in **A**, and they demonstrate how the red curves in **B** were associated with longer saccadic eye displacements than in control. **(C, D)** Radial eye velocity traces for the same eye movements in **A**, **B** (but plotting data only from saccade onset this time). Faint curves show individual trials, and thick curves denote the across-trial averages. Electrical pulses at saccade onset clearly resulted in a subsequent prolongation of ongoing saccades, evident as a secondary velocity pulse approximately 30 ms later (**D**). Figure S6 shows that 3 pulses alone (without an ongoing plan) were not sufficient to evoke a saccadic eye movement.

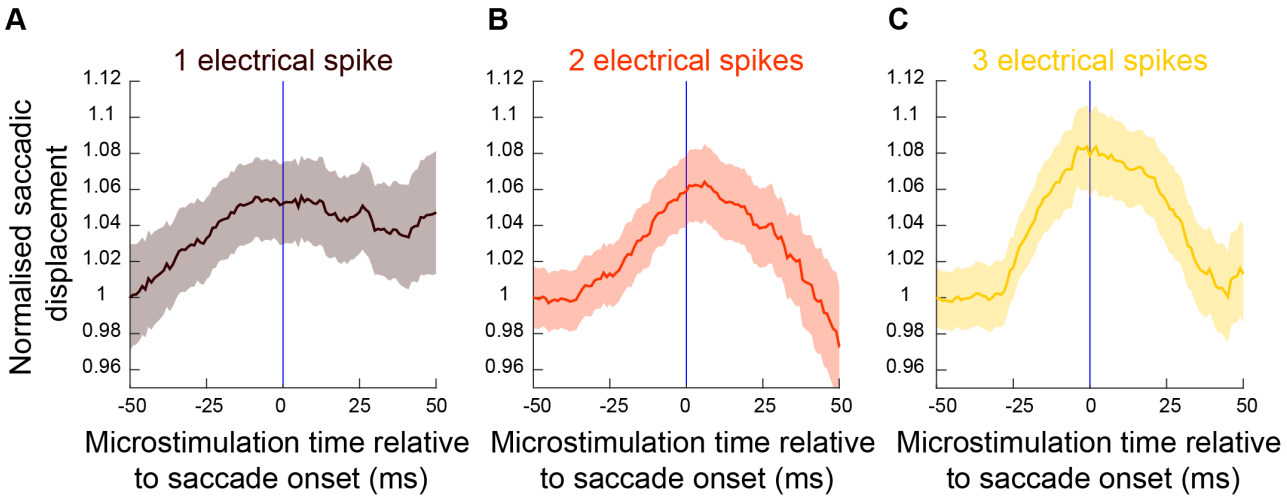

Figure 8 Peri-saccadic electrical microstimulation with 1, 2, or 3 spikes alters saccade metrics. Time courses of saccadic displacement as a function of peri-saccadic microstimulation. We measured the total saccadic displacement (0-100 ms from saccade onset) as a function of the time of electrical microstimulation that was applied peri-saccadically. Amplitude displacements were normalized to the measured displacement when microstimulation was far from saccade onset (i.e. averaged across ±25 ms centered on 50 ms before saccade onset). Each panel shows results with 1 (**A**), 2 (**B**), or 3 (**C**) peri-saccadic electrical microstimulation pulses applied to the SC at a site more eccentric than the saccade target location (but along a similar vector direction). Single pulse microstimulation had a modest impact on the eye displacement, and it was loosely centered around saccade onset. With double and triple pulse microstimulation variants, the alteration was significantly stronger and clearly centered in a precise time window around the saccade. This time window was highly consistent with the time window of Fig. 6A with “visual” injected spikes that altered microsaccade metrics. Error bars denote 95% confidence intervals.

Discussion

We experimentally injected movement-unrelated spiking activity into the SC map at the time of saccade generation. We found that such activity was sufficient to significantly alter the metrics of the generated saccadic eye movement, suggesting an instantaneous readout of the entire SC map for implementing any individual movement.

Our results reveal a component of motor variability that we believe has been previously unaccounted for, namely, the fact that ever-present spiking activity in the entire SC map (whether due to sustained firing rates for a stimulus presented in the RF, like in our first experiment, or otherwise) can “leak” into the readout performed by downstream motor structures when executing a movement. In fact, our results from Fig. 6C showed that any intra-saccadic spikes on the SC map (far from the location of the motor burst) were sufficient to modulate microsaccade metrics, meaning that there was no need for a stimulus onset or even a stimulus-driven visual burst, like in Figs. 3-6, to give rise to our observations. Indeed, saccades during natural viewing show an immense amount of kinematic variability when compared to simplified laboratory tasks with only a single saccade target (Berg et al., 2009). In such natural viewing, natural images with plenty of low spatial frequency image power are expected to strongly activate a large number of SC neurons, which prefer low spatial frequencies, around the time of saccades (Chen et al., 2018; Khademi et al., 2020).

From an ecological perspective, our results demonstrate a remarkable flexibility of the oculomotor system during eye movement generation. Historically, saccades were thought to be controlled by an open-loop control system due to their apparent ballistic nature. However, other evidence, including our current results, clearly showed that individual saccades are actually malleable brain processes. In our case, we experimentally tried to generate a movement-unrelated “visual” or “electrical” burst of activity that precisely coincided with the time of saccade triggering. We uncovered an instantaneous readout of the entire SC map that includes all the activity related to the ongoing motor program as well

527 as the “extra” activity. In real life, this extra activity might happen due to external sensory
528 stimulation, such as the presence of a new object in the visual scene.

529 Such integration of sensory signals into the motor plan was also not merely a “loose”
530 leakage phenomenon; rather, it exhibited a lawful additive process between the “visual”
531 spikes injected into the SC population and the altered microsaccade amplitudes (Figs. 4, 6).
532 The more “visual” spikes that occurred intra-saccadically, the larger the microsaccades
533 became, following a linear relationship. We discount the possibility that this effect was due
534 to movement-related bursts per se, because we ensured that the neurons that we recorded
535 from were not exhibiting movement bursts for the ranges of eye movements that we
536 analyzed (Fig. S1). We suggest that this additive mechanism might underlie many of the
537 effects commonly seen in experimental psychophysics, in which saccade kinematics are
538 systematically altered by the presence of sudden irrelevant visual information available as
539 close as 40 ms to movement onset (Edelman and Xu, 2009; Buonocore and McIntosh, 2012;
540 Guillaume, 2012; Buonocore et al., 2016; Buonocore et al., 2017b; Malevich et al., 2020a).
541 Our hypothesis is that these modulations are a behavioral manifestation of the
542 instantaneous readout of the activity on the SC map, as we also previously hypothesized
543 (Hafed and Ignashchenkova, 2013; Buonocore et al., 2017b). Moreover, similar specification
544 mechanisms can be seen in the instantaneous alteration of eye velocity during smooth
545 pursuit when small flashes are presented (Buonocore et al., 2019), and even with ocular
546 position drift during fixation (Malevich et al., 2020b). These observations extend the
547 mechanisms uncovered in our study to the pursuit system and beyond, and they also relate
548 to sequential activation of SC neurons during curved saccades associated with planning
549 sequences of movements (Port and Wurtz, 2003).

550 Our investigations, which were driven by behavioral modulations observed in
551 psychophysical experiments as alluded to above, therefore now provide a means to
552 precisely quantify such behavioral modulations when sensory stimuli arrive in close temporal

553 proximity to saccade generation. They also extend situations in which concurrent saccade
554 motor plans can give rise to vector averaging (Robinson, 1972; Schiller et al., 1979; Schiller
555 and Sandell, 1983; Sparks and Mays, 1983; Edelman and Keller, 1998; Katnani and Gandhi,
556 2011) or curved (McPeek et al., 2003) saccades to ones in which a sensory burst itself is
557 what is concurrently present with the saccade motor program. In that sense, the sensory
558 burst may act as a motor program itself. This is similar to studies of express saccades,
559 having ultra-short latencies that appear to merge visual and motor bursts in the SC (Edelman
560 and Keller, 1996; Sparks et al., 2000). In these saccades, it could be that the triggering for
561 the saccades happens exactly at the time of the visual bursts, therefore "pulling" the
562 saccades to the locations of the bursts. This is not unlike our observations (Figs. 3-6), and
563 can nicely explain why early microsaccades shortly after stimulus onset not only are
564 congruent with the stimulus location, but are also larger in size than usual (Hafed and
565 Ignashchenkova, 2013; Buonocore et al., 2017b).

566 Most intriguingly, our results motivate similar neurophysiological studies on sensory-
567 motor integration in other oculomotor structures. For example, our own ongoing experiments
568 in the lower oculomotor brainstem, at the very final stage for saccade control (Keller, 1974;
569 Büttner-Ennever et al., 1988; Gandhi and Keller, 1999b; Missal and Keller, 2002), are
570 revealing highly thought provoking visual pattern analysis capabilities of intrinsically motor
571 neurons (Buonocore et al., 2020). These and other experiments will, in the future, clarify the
572 mechanisms behind multiplexing of visual and motor processing in general, across other
573 subcortical areas, like pulvinar, and also cortical areas, like FEF and LIP. Moreover, these
574 sensory-motor integration processes can have direct repercussions on commonly used
575 behavioral paradigms in which microsaccades and saccades happen around the time of
576 attentional cues/probes and can alter performance (Hafed, 2013; Hafed et al., 2015; Tian et
577 al., 2016; Buonocore et al., 2017b).

578 Our electrical microstimulation manipulations are also interesting because they add
579 to what we believe is already strong causal evidence from our visual burst manipulations.
580 While previous studies have demonstrated the possibility to terminate the current saccadic
581 motor plan in favor of a new one by electrical microstimulation of the SC (Gandhi and Keller,
582 1999a), our experiments rather focused on the flexibility of "leaking" extra subtle activity into
583 the ongoing oculomotor plan. As such, we used low currents, and we microstimulated peri-
584 saccadically at more eccentric locations than the generated saccades, unlike in the earlier
585 studies. Our experiments therefore complement these earlier reports performing SC
586 electrical microstimulation.

587 Consistent with the above sentiment, our study generally illuminates emerging and
588 classic models of the role of the SC in saccade control. In a recent model by Goossens and
589 Van Opstal (2006), it was suggested that every SC spike during a motor burst contributes a
590 mini-vector of eye movement tendency, such that the aggregate sum of movement
591 tendencies comprises the overall trajectory. Our results are consistent with this model, and
592 related ones also invoking a role of SC activity levels in instantaneous trajectory control
593 (Waitzman et al., 1991; Ivan et al., 2018), in the sense that we did observe linear
594 contributions of additional SC spikes on eye movement metrics (Figs. 4, 6). However, as
595 stated in Introduction, our results add to this model the notion that there need not be a
596 "classifier" identifying particular SC spikes as being the movement-related spikes of the
597 current movement and other spikes as being irrelevant. More importantly, we found
598 diminishing returns of relative eccentricity between the "extra" spikes and the current motor
599 burst (Figs. 3, S3, 4, S5). According to their model, the more eccentric spikes that we
600 introduced from more eccentric neurons should have each contributed "mini-vectors" that
601 were actually larger than the "mini-vectors" contributed by the less eccentric spikes from the
602 less eccentric neurons. So, if anything, we should have expected larger effects for the more
603 eccentric neurons. This was clearly not the case. Therefore, this model needs to consider

local and remote interactions more explicitly. The model also needs to consider other factors like input from other areas. Indeed, Peel et al. (2019) reported that the SC generates fewer saccade-related spikes during FEF inactivation, even for matched saccade amplitudes. Similarly, we recently found that microsaccades without visual guidance can be associated with fewer active SC neurons than similarly-sized microsaccades with visual guidance, because of so-called visually-dependent saccade-related neurons (Willeke et al., 2019). Finally, SC motor bursts themselves are very different for saccades directed to upper versus lower visual field locations, without an apparent difference in saccade kinematics (Hafed and Chen, 2016). All of these observations suggest that further research on the SC contributions to saccade trajectory control is strongly needed.

In all, we believe that our results expose highly plausible neural mechanisms associated with robust behavioral effects on saccades accompanied by nearby visual flashes in a variety of paradigms, and they also motivate revisiting a classic neurophysiological problem, the role of the SC in saccade control, from the perspective of visual-motor multiplexing within individual brain circuits, and even individual neurons themselves.

Acknowledgements

We were funded by the Deutsche Forschungsgemeinschaft (DFG) through the Research Unit: FOR1847 (project: HA6749/2-1). We were also funded by the Werner Reichardt Centre for Integrative Neuroscience (CIN; DFG EXC307) and the Hertie Institute for Clinical Brain Research.

Declaration of interests

The authors declare no competing interests.

Author contributions

AB, MPB, ZMH performed the microstimulation experiments. AB, ZMH analyzed the recording data. AB, MPB, ZMH analyzed the microstimulation data. AB, MPB, ZMH wrote and edited the manuscript.

Methods

Animal preparation

We collected data from three (M, N, and P) adult, male rhesus monkeys (Macaca mulatta) that were 6-8 years of age and weighed 6-8 kg. The experiments were approved (licenses: CIN3/13; CIN4/19G) by ethics committees at the regional governmental offices of the city of Tuebingen and were in accordance with European Union guidelines on animal research and the associated implementations of these guidelines in German law. The monkeys were prepared using standard surgical procedures necessary for behavioral training and intracranial recordings. In short, monkeys N and P had a chamber centered on the midline and aiming at the superior colliculus (SC) with an angle of 35 and 38 degrees posterior of vertical in the sagittal plane, respectively. Monkey M was implanted with a similar chamber having an angle of 38 degrees posterior of vertical in the sagittal plane. The details of the surgical procedures were described in previous reports (monkeys N and P: Chen and Hafed, 2013; Monkey M: Willeke et al., 2019). To record eye movements with high temporal and spatial precision, all monkeys were also implanted with a scleral search coil. This allowed eye tracking using the magnetic induction technique (Fuchs and Robinson, 1966; Judge et al., 1980). Monkeys N and P were each implanted in the right and left eye, respectively. Monkey M was implanted in both eyes.

Experimental control system and monkey setup

We used a custom-built real-time experimental control system that drove stimulus presentation and ensured monkey behavioral monitoring and reward delivery. It also controlled an electrical microstimulation device (Stimpulse; FHC, Inc.) to trigger microstimulation. The details of the system are reported in recent publications (Chen and Hafed, 2013; Tian et al., 2016).

660 During the testing sessions, the animals were head fixed and seated in a standard
661 primate chair placed at a distance of 74 cm from a CRT monitor. The eye height was aligned
662 with the center of the screen. The room was completely dark with the only light source being
663 the monitor. All stimuli were presented over a uniform gray background (Monkey M: 29.7
664 Cd/m^2; Monkeys N and P: 21 Cd/m^2). In all the experiments, the fixation spot consisted in a
665 small square made of 3 by 3 pixels (about 8.5 by 8.5 min arc) colored in white (Monkey M:
666 86 Cd/m^2; Monkeys N and P: 72 Cd/m^2). The central pixel had the same color as the
667 background.
668
669 *Behavioral tasks and electrophysiology*
670 *Experiment 1: injecting visual spikes at the time of saccade generation*
671 We performed a novel analysis of SC data reported on earlier; our behavioral task is
672 therefore described in detail in (Chen et al., 2015). Briefly, we used a fixation paradigm
673 during which we introduced a peripheral transient visual event at random intervals (see Fig.
674 1A). Each trial started with a white fixation spot presented at the center of the display over
675 a uniform gray background. The monkey was required to align its gaze with the fixation spot.
676 Because fixation is an active process, this steady-state fixation paradigm allowed us to have
677 a scenario in which microsaccades were periodically generated (Hafed and
678 Ignashchenkova, 2013). After a random interval, we presented a stimulus consisting of a
679 vertical sine wave grating of 2.2 cycles/deg spatial frequency and filling the visual response
680 field (RF) of the recorded neuron. The stimulus onset allowed experimentally injecting visual
681 spikes into the SC at retinotopic locations dissociated from the neurons involved in
682 microsaccade generation (Hafed et al., 2009; Willeke et al., 2019). Therefore, we could
683 investigate the influence of such injected spiking activity if it happened to occur in the middle
684 of an ongoing microsaccade (see Results). We varied the contrast of the grating across trials
685 in order to vary the amount of injected SC spiking activity around the time of microsaccade

686 generation. Specifically, grating contrast could be one of 5%, 10%, 20%, 40%, or 80% (Chen
687 et al., 2015). For the current study, we only analyzed trials with the highest 3 contrasts. We
688 related microsaccade kinematics to injected "visual" spiking activity. Overall, we analyzed
689 84 SC visual (44) and visual-motor (40) neurons in two monkeys (N and P).
690
691 *Experiment 2: injecting electrical spikes at the time of saccade generation*
692 In monkey M, we performed peri-saccadic electrical microstimulation of the SC during a
693 visually-guided saccade task (Fig. 1C). That is, rather than peri-saccadic spiking activity
694 induced in the SC by visual onsets, we electrically microstimulated the SC around the time
695 of saccade generation.
696 Before each session, we first identified the direction and amplitude of the visual field
697 location associated with the electrode position in the SC topographic map. We did so by
698 mapping the visual and movement RF's encountered by the electrode using a standard
699 delayed visually-guided saccade task (Chen et al., 2015). In a second step, we confirmed
700 the electrode location by assessing the size and direction of the saccade vector evoked
701 through electrical microstimulation (our electrodes had relatively low impedances of <1
702 MOhm, and they were placed in the intermediate layers of the SC). We programmed the
703 microstimulation parameters of a given test on the Stimpulse (FHC, Inc.) system's user
704 interface, and we then triggered the microstimulation train using our real-time experiment
705 control system. While the monkey was maintaining fixation on a continuously visible fixation
706 spot, we microstimulated the SC with symmetric biphasic current pulses having an amplitude
707 of 30-45 μA and inter-pulse interval of 3.3 ms (i.e. pulse train frequency of 300Hz). The pulse
708 train duration was relatively short (70-150 ms), and each individual pulse consisted of a 150
709 μs cathodal phase followed immediately by a 150 μs anodal phase. Such electrical
710 microstimulation reliably elicited short-latency eye movements of a particular size and
711 direction (Fig. S6A).

712 Once the RF's of the neurons at the SC site were established using both recording and
713 microstimulation, as per the above procedures, we started the main experiment, which
714 consisted of a simple visually-guided saccade task. The monkey fixated, and the fixation
715 spot was then removed with a simultaneous presentation of a visual target in the periphery
716 (white circle of 0.45 deg radius). We chose the location of the visual target such that it was
717 not overlapping with the RF's of the neurons that we microstimulated earlier. Specifically,
718 the location of the target stimulus was chosen to be about halfway between the fixation spot
719 and the RF locations being microstimulated on the SC map. Thus, when we injected
720 "electrical" stimuli into the SC, we were injecting activity at a site that was spatially
721 dissociated from the saccade target location; this is conceptually the same as the situation
722 in the "visual" spike experiments above (Fig. 1A, B). In different blocks, we injected either 1,
723 2, or 3 electrical pulses into the SC peri-saccadically. Pulse amplitude currents were similar
724 to above, and inter-pulse intervals (for double and triple pulse microstimulation) were 3.3
725 ms. To achieve peri-saccadic microstimulation, as in peri-saccadic visual presentation
726 experiments (e.g. Buonocore et al., 2017a; Grujic et al., 2018), we randomized the time of
727 microstimulation from trial to trial. Specifically, each trial started with an initial fixation interval
728 of approximately 300-700 ms. When the saccade target appeared, we introduced a random
729 delay between approximately 70 ms and 170 ms (uniform distribution) before injecting
730 electrical spikes. Given typical visually-guided saccade reaction times, this resulted in
731 electrical microstimulation pulses appearing either well before, during, or well after saccade
732 onset. This, in turn, allowed us to assess the effects of peri-saccadic single, double, or triple
733 pulse microstimulation in the SC (Fig. 6 in Results). In a separate control block, we
734 confirmed that 3 pulses electrically injected into the SC (with the same parameters as in the
735 main experiment) during simple fixation did not elicit any systematic eye movements (Fig.
736 S6B, C). Thus, whatever impacts that we had on visually-guided saccade metrics were not
737 due to an explicitly evoked saccade caused by electrical microstimulation.

Data analysis

All analyses were performed with custom scripts in Matlab (MathWorks, Inc.). Most of the analyses involving grouping the eye movement data into groups of movements going either towards or opposite a recorded neuron's RF. To make this classification, we first calculated the angle of the RF relative to the fixation spot. Then, all eye movements with an angle ±90 degrees around the RF direction were classified as being "towards" the RF. All remaining eye movements were classified as being directed "opposite" to the RF. Movement angles were defined as the arctangent subtended by the horizontal and vertical component between movement onset and end. RF angles were defined as the arctangent subtended by the horizontal and vertical coordinates of the RF locations relative to the fixation spot.

To analyze peak firing rates "without saccades" (Figs. 2, 3B, S2, S3B), we selected all trials in which there were no microsaccades btween -100 ms and 200 ms relative to stimulus onset. We then averaged all the firing rates across trials, and we determined the peak firing rate for each neuron from the across-trial average curve. For the peak firing rate "with saccades", we took all the trials in which a microsaccade was either starting or ending during the so-called visual burst interval, which we defined to be the interval 30-100 ms after stimulus onset. Paired-sample t-tests were performed to test the influence of saccades on the peak visual burst with an α level of 0.05 unless otherwise stated (Figs. 2, S2).

To summarize the time courses of microsaccade amplitudes after stimulus onset (Figs. 3A, S3A), we selected the first saccade of each trial that was triggered within the interval from -100 ms to +150 ms relative to stimulus onset. All the microsaccade amplitudes were then pooled together across monkeys and sessions. The microsaccade amplitude time course was obtained by filtering the data with a running average window of 50 ms with a step size of 10 ms. To statistically test the effect of grating contrasts on these time courses, we performed a one-way ANOVA on saccade amplitudes for all saccades occurring between 50 ms and 100 ms after stimulus onset. To compare the effect of grating contrast on SC

764 visual bursts (Figs. 3B, S3B), for each neuron, we normalized the firing rate based on the
765 maximum firing rate elicited by the strongest contrast. Subsequently, we calculated the
766 mean firing rate of the population and the 95% confidence interval for the different contrast
767 levels. Both the amplitude and the firing rate analyses focused on the three highest contrasts
768 because the first two contrast levels did not have a visible impact on eye movement
769 behavior.

770 For some analyses (Figs. 4-6, S5), we explored the relationship between the number
771 of spikes emitted by a recorded neuron and saccade amplitude. This allowed us to directly
772 investigate the effect of each single additional spike per recorded neuron in the SC map on
773 an ongoing saccade, irrespective of other variables. We selected all the trials in which an
774 eye movement was performed in the direction of the grating soon after its presentation. The
775 analysis was restricted to the three highest contrasts, since they had a clear effect on the
776 eye movement behavior (Fig.3A). For each selected saccade, we counted the number of
777 spikes happening from a given recorded neuron between movement onset movement peak
778 velocity. For Figs. 4A, S5A, we calculated the "radial eye position" from saccade start as the
779 Euclidian distance of any eye position sample (i.e. at any millisecond) recorded during an
780 eye movement relative to the eye position at movement onset (see for similar procedures:
781 Hafed et al., 2009; Buonocore et al., 2017b). To make statistical inferences on the effects
782 of the number of spikes on saccade amplitude (Figs. 4B, S5B), we proceeded by fitting a
783 generalized linear model to the raw data with equation: $y = \beta_0 + \beta_1 * x$ where 'x' was our
784 predictor variable, the number of spikes, and 'y' was the predicted amplitude. The
785 parameters fitted were: β_0 the intercept, β_1 the slope. We imposed a cutoff of at least 15
786 trials for each level of the predictor, leading to exclusion of spike counts bigger than six.

787 To study the time window of influence of each added spike on saccade amplitudes
788 (Figs. 5, 6), we generated raster plots from all trials of all sessions by aligning each spike
789 raster trace to the saccade occurring on the same trial (either saccade start, peak velocity,

or end). The saccades were chosen as those that happened after stimulus onset, and the alignment was based on the time of peak visual burst after stimulus onset on a given trial relative to the time of the movement. We selected data from the three highest stimulus contrasts and also with eye movements directed towards the RF, since the modulation in behavior was most pronounced in these cases (e.g. Fig. 4). To identify the point at which the amplitude diverged from a baseline level in Fig. 5D, we first sorted all the amplitudes based on burst time relative to saccade onset (Fig. 5A). Then, we made bins of 30 trials each from which we derived the mean amplitude values (Fig. 5D). We also tested the amplitudes of each bin against the first one (baseline amplitude) to determine when the amplitude increase was significant. To do so, we performed two-sample independent t-tests between each pair, and we adjusted the alpha level with Bonferroni correction. We chose as an index for a significant increase in amplitude the point at which three consecutive bins were significantly different from the baseline (first horizontal blue line in the trial sorting of Fig. 5D). The next three consecutive bins that did not differ anymore from the baseline indicated that the amplitude increase was not significant anymore (second horizontal blue line in the trial sorting of Fig. 5D).

For the microstimulation experiment, we first ensured that the monkey was maintaining stable fixation in an interval between -50 ms to 300 ms around target onset and that the eyes were within a fixation window of one degree radius. We then selected as response saccades all the eye movements made 75 ms to 400 ms after target appearance and with an amplitude larger than halfway between fixation and target location. Such strict criteria were used because the target could have been placed in relatively rostral regions, where microsaccades happen frequently and might therefore interfere with the goal directed saccade. Subsequently, on the selected saccade, we calculated the “eye displacement” as the radial position of the eyes from saccade start to 100 ms thereafter. This value was then normalized by the average displacement obtained with microstimulation in a time window of

816 ±25 ms centered on 50 ms before movement onset (i.e. well before the onset of our
817 behavioral effect) to allow the pooling of different sessions that had different target
818 eccentricities. The eye displacement curve (Fig. 8) was calculated by binning the eye
819 displacement values in a time interval of 50 ms before to 100 ms after saccade onset, with
820 a bin size of 50 ms and a step of 1 ms. This procedure was repeated independently for the
821 1, 2, or 3 spike blocks.
822

References

Alexander GE, Crutcher MD (1990) Neural representations of the target (goal) of visually guided arm movements in three motor areas of the monkey. J Neurophysiol 64:164-178.

Berg DJ, Boehnke SE, Marino RA, Munoz DP, Itti L (2009) Free viewing of dynamic stimuli by humans and monkeys. J Vis 9:19.11-15.

Breveglieri R, Bosco A, Galletti C, Passarelli L, Fattori P (2016) Neural activity in the medial parietal area V6A while grasping with or without visual feedback. Sci Rep 6:28893.

Bruce CJ, Goldberg ME (1985) Primate frontal eye fields. I. Single neurons discharging before saccades. Journal of Neurophysiology 53:603-635.

Buonocore A, McIntosh RD (2012) Modulation of saccadic inhibition by distractor size and location. Vision Research 69:32-41.

Buonocore A, McIntosh RD, Melcher D (2016) Beyond the point of no return: effects of visual distractors on saccade amplitude and velocity. Journal of Neurophysiology 115:752-762.

Buonocore A, Fracasso A, Melcher D (2017a) Pre-saccadic perception: Separate time courses for enhancement and spatial pooling at the saccade target. PLoS ONE 12:e0178902-0178923.

Buonocore A, Skinner J, Hafed ZM (2019) Eye Position Error Influence over “Open-Loop” Smooth Pursuit Initiation. The Journal of Neuroscience 39:2709-2721.

Buonocore A, Baumann MP, Hafed ZM (2020) Visual pattern analysis by motor neurons (Abstract). Computational and Systems Neuroscience (Cosyne) 147.

Buonocore A, Chen C-Y, Tian X, Idrees S, Münch TA, Hafed ZM (2017b) Alteration of the microsaccadic velocity-amplitude main sequence relationship after visual transients: implications for models of saccade control. Journal of Neurophysiology 117:1894-1910.

Büttner-Ennever JA, Cohen B, Pause M, Fries W (1988) Raphe nucleus of the pons containing omnipause neurons of the oculomotor system in the monkey, and its homologue in man. Journal of Comparative Neurology 267:307-321.

Chen CY, Hafed ZM (2013) Postmicrosaccadic Enhancement of Slow Eye Movements. Journal of Neuroscience 33:5375-5386.

Chen CY, Ignashchenkova A, Thier P, Hafed ZM (2015) Neuronal Response Gain Enhancement prior to Microsaccades. Current Biology 25:2065-2074.

Chen CY, Hoffmann KP, Distler C, Hafed ZM (2019) The Foveal Visual Representation of the Primate Superior Colliculus. Curr Biol 29:2109-2119 e2107.

Chen CY, Sonnenberg L, Weller S, Witschel T, Hafed ZM (2018) Spatial frequency sensitivity in macaque midbrain. Nature Communications 9:2852.

Cynader M, Berman N (1972) Receptive-field organization of monkey superior colliculus. J Neurophysiol 35:187-201.

Edelman JA, Keller EL (1996) Activity of visuomotor burst neurons in the superior colliculus accompanying express saccades. Journal of Neurophysiology 76:908-926.

Edelman JA, Keller EL (1998) Dependence on target configuration of express saccade-related activity in the primate superior colliculus. J Neurophysiol 80:1407-1426.

Edelman JA, Goldberg ME (2001) Dependence of Saccade-Related Activity in the Primate Superior Colliculus on Visual Target Presence. Journal of Neurophysiology 86:676-691.

Edelman JA, Xu KZ (2009) Inhibition of Voluntary Saccadic Eye Movement Commands by Abrupt Visual Onsets. Journal of Neurophysiology 101:1222-1234.

Fuchs AF, Robinson DA (1966) A method for measuring horizontal and vertical eye movement chronically in the monkey. J Appl Physiol 21:1068-1070.
Gandhi NJ, Keller EL (1999a) Comparison of Saccades Perturbed by Stimulation of the Rostral Superior Colliculus, the Caudal Superior Colliculus, and the Omnipause Neuron Region. Journal of Neurophysiology 82:3236-3253.
Gandhi NJ, Keller EL (1999b) Activity of the brain stem omnipause neurons during saccades perturbed by stimulation of the primate superior colliculus. Journal of Neurophysiology 82:3254-3267.
Goldberg ME, Wurtz RH (1972a) Activity of superior colliculus in behaving monkey. II. Effect of attention on neuronal responses. J Neurophysiol 35:560-574.
Goldberg ME, Wurtz RH (1972b) Activity of superior colliculus in behaving monkey. I. Visual receptive fields of single neurons. J Neurophysiol 35:542-559.
Goossens HH, Van Opstal AJ (2006) Dynamic ensemble coding of saccades in the monkey superior colliculus. J Neurophysiol 95:2326-2341.
Goossens HHLM, Van Opstal AJ (2012) Optimal Control of Saccades by Spatial-Temporal Activity Patterns in the Monkey Superior Colliculus. PLoS Computational Biology 8:e1002508.
Grujic N, Brehm N, Gloge C, Zhuo W, Hafed ZM (2018) Perisaccadic perceptual mislocalization is different for upward saccades. J Neurophysiol 120:3198-3216.
Guillaume A (2012) Saccadic inhibition is accompanied by large and complex amplitude modulations when induced by visual backward masking. Journal of Vision 12:5-5.
Hafed ZM (2011) Mechanisms for generating and compensating for the smallest possible saccades. European Journal of Neuroscience 33:2101-2113.
Hafed ZM (2013) Alteration of Visual Perception prior to Microsaccades. Neuron 77:775-786.
Hafed ZM, Krauzlis RJ (2012a) Similarity of superior colliculus involvement in microsaccade and saccade generation. Journal of Neurophysiology 107:1904-1916.
Hafed ZM, Krauzlis RJ (2012b) Similarity of superior colliculus involvement in microsaccade and saccade generation. J Neurophysiol 107:1904-1916.
Hafed ZM, Ignashchenkova A (2013) On the Dissociation between Microsaccade Rate and Direction after Peripheral Cues: Microsaccadic Inhibition Revisited. Journal of Neuroscience 33:16220-16235.
Hafed ZM, Chen CY (2016) Sharper, Stronger, Faster Upper Visual Field Representation in Primate Superior Colliculus. Curr Biol 26:1647-1658.
Hafed ZM, Goffart L, Krauzlis RJ (2009) A Neural Mechanism for Microsaccade Generation in the Primate Superior Colliculus. Science (New York, NY) 323:940-943.
Hafed ZM, Chen C-Y, Tian X (2015) Vision, Perception, and Attention through the Lens of Microsaccades: Mechanisms and Implications. Frontiers in Systems Neuroscience 9:779.
Honda H (1989) Perceptual localization of visual stimuli flashed during saccades. Perception & Psychophysics 45:162-174.
Ivan S, Uday KJ, Neeraj JG (2018) Instantaneous Midbrain Control of Saccade Velocity. The Journal of Neuroscience 38:10156-10167.
Judge SJ, Richmond BJ, Chu FC (1980) Implantation of magnetic search coils for measurement of eye position: an improved method. Vision Res 20:535-538.
Katnani HA, Gandhi NJ (2011) Order of operations for decoding superior colliculus activity for saccade generation. Journal of Neurophysiology 106:1250-1259.
Katnani HA, Gandhi NJ (2012) The relative impact of microstimulation parameters on movement generation. Journal of Neurophysiology 108:528-538.

Keller EL (1974) Participation of Medial Pontine Reticular-Formation in Eye-Movement Generation in Monkey. Journal of Neurophysiology 37:316-332.
Khademi F, Chen CY, Hafed ZM (2020) Visual feature tuning of superior colliculus neural reafferent responses after fixational microsaccades. J Neurophysiol 123:2136-2153.
Krekelberg B, Kubischik M, Hoffmann KP, Bremmer F (2003) Neural correlates of visual localization and perisaccadic mislocalization. Neuron 37:537-545.
Lappe M, Awater H, Krekelberg B (2000) Postsaccadic visual references generate presaccadic compression of space. Nature 403:892-895.
Li X, Basso MA (2008) Preparing to move increases the sensitivity of superior colliculus neurons. J Neurosci 28:4561-4577.
Malevich T, Buonocore A, Hafed ZM (2020a) Dependence of the stimulus-driven microsaccade rate signature on visual stimulus polarity. bioRxiv:2020.2005.2023.112417.
Malevich T, Buonocore A, Hafed ZM (2020b) Rapid stimulus-driven modulation of slow ocular position drifts. bioRxiv:2020.2004.2002.022335.
Mays LE, Sparks DL (1980) Dissociation of visual and saccade-related responses in superior colliculus neurons. J Neurophysiol 43:207-232.
Mazzoni P, Bracewell RM, Barash S, Andersen RA (1996) Motor intention activity in the macaque's lateral intraparietal area. I. Dissociation of motor plan from sensory memory. J Neurophysiol 76:1439-1456.
McPeek RM, Han JH, Keller EL (2003) Competition between saccade goals in the superior colliculus produces saccade curvature. J Neurophysiol 89:2577-2590.
Missal M, Keller EL (2002) Common inhibitory mechanism for saccades and smooth-pursuit eye movements. Journal of Neurophysiology.
Miyashita N, Hikosaka O (1996) Minimal synaptic delay in the saccadic output pathway of the superior colliculus studied in awake monkey. Exp Brain Res 112:187-196.
Mohler CW, Wurtz RH (1976) Organization of monkey superior colliculus: intermediate layer cells discharging before eye movements. J Neurophysiol 39:722-744.
Morrone MC, Ross J, Burr DC (1997) Apparent position of visual targets during real and simulated saccadic eye movements. Journal of Neuroscience 17:7941-7953.
Munoz DP, Wurtz RH (1995) Saccade-related activity in monkey superior colliculus. I. Characteristics of burst and buildup cells. Journal of Neurophysiology 73:2313-2333.
Munoz DP, Waitzman DM, Wurtz RH (1996) Activity of neurons in monkey superior colliculus during interrupted saccades. Journal of Neurophysiology 75:2562-2580.
Peel TR, Dash S, Lomber SG, Corneil BD (2019) Frontal eye field inactivation alters the readout of superior colliculus activity for saccade generation in a task-dependent manner. bioRxiv:646604.
Port NL, Wurtz RH (2003) Sequential activity of simultaneously recorded neurons in the superior colliculus during curved saccades. J Neurophysiol 90:1887-1903.
Robinson DA (1972) Eye movements evoked by collicular stimulation in the alert monkey. Vision Res 12:1795-1808.
Ross J, Morrone MC, Burr DC (1997) Compression of visual space before saccades. Nature 386:598-601.
Schall J, Hanes D, Thompson K, King D (1995) Saccade target selection in frontal eye field of macaque. I. Visual and premovement activation. The Journal of Neuroscience 15:6905-6918.
Schall JD, Hanes DP (1993) Neural basis of saccade target selection in frontal eye field during visual search. Nature 366:467-469.

Schiller PH, Sandell JH (1983) Interactions between visually and electrically elicited saccades before and after superior colliculus and frontal eye field ablations in the rhesus monkey. Exp Brain Res 49:381-392.

Schiller PH, True SD, Conway JL (1979) Paired stimulation of the frontal eye fields and the euperior colliculus of the rhesus monkey. Brain Res 179:162-164.

Shen L, Alexander GE (1997) Neural correlates of a spatial sensory-to-motor transformation in primary motor cortex. J Neurophysiol 77:1171-1194.

Sparks D, Rohrer WH, Zhang Y (2000) The role of the superior colliculus in saccade initiation: a study of express saccades and the gap effect. Vision Res 40:2763-2777.

Sparks DL, Mays LE (1983) Spatial localization of saccade targets. I. Compensation for stimulation-induced perturbations in eye position. J Neurophysiol 49:45-63.

Stanford TR, Freedman EG, Sparks DL (1996) Site and parameters of microstimulation: evidence for independent effects on the properties of saccades evoked from the primate superior colliculus. Journal of Neurophysiology 76:3360-3381.

Tehovnik EJ, Sommer MA, Chou IH, Slocum WM, Schiller PH (2000) Eye fields in the frontal lobes of primates. Brain Res Brain Res Rev 32:413-448.

Tian X, Yoshida M, Hafed ZM (2016) A Microsaccadic Account of Attentional Capture and Inhibition of Return in Posner Cueing. Frontiers in Systems Neuroscience 10.

Van Opstal AJ, Goossens HHLM (2008) Linear ensemble-coding in midbrain superior colliculus specifies the saccade kinematics. Biological cybernetics 98:561-577.

Waitzman DM, Ma TP, Optican LM, Wurtz RH (1991) Superior colliculus neurons mediate the dynamic characteristics of saccades. Journal of Neurophysiology 66:1716-1737.

Willeke KF, Tian X, Buonocore A, Bellet J, Ramirez-Cardenas A, Hafed ZM (2019) Memory-guided microsaccades. Nature Communications 10:3710.

Wurtz RH, Goldberg ME (1972) Activity of superior colliculus in behaving monkey. 3. Cells discharging before eye movements. J Neurophysiol 35:575-586.

Wurtz RH, Albano JE (1980) Visual-motor function of the primate superior colliculus. Annu Rev Neurosci 3:189-226.

Supplementary figures

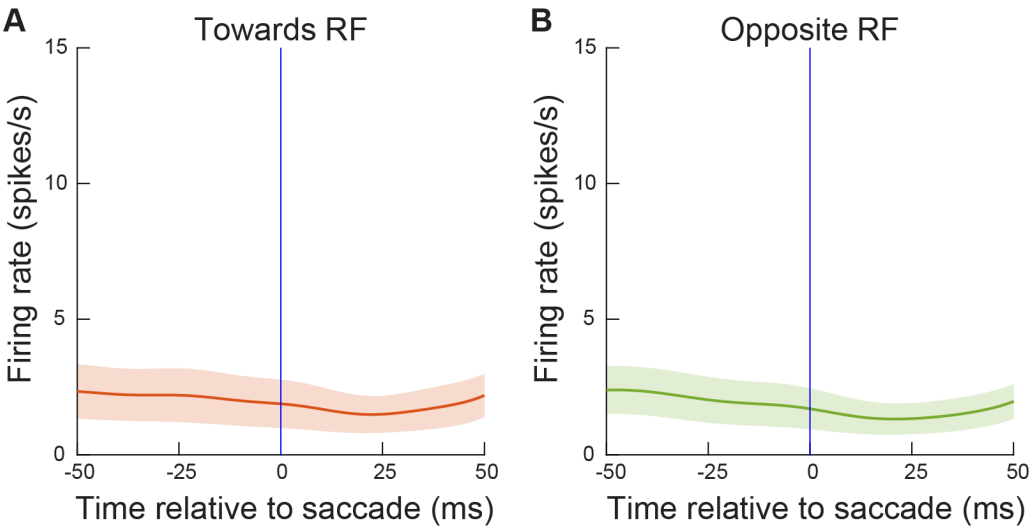

Figure S1 Injected "visua" spikes in our experiments were in neurons that were not directly involved in generating the saccades that were being altered in our main analyses of Figs. 2-6. Mean firing rate of all of our neurons aligned to saccade onset (blue line) for eye movements made towards the RF (**A**, orange) or opposite it (**B**, green). The movements were all selected during a baseline pre-stimulus period (-100 to -25 ms from stimulus onset) in the absence of any visual stimuli inside the RF's. Error bars denote 95% confidence intervals. The neurons did not show any bursts for microsaccade generation, confirming that we were only measuring visual bursts and not concurrent movement-related activity in Figs. 2-6.

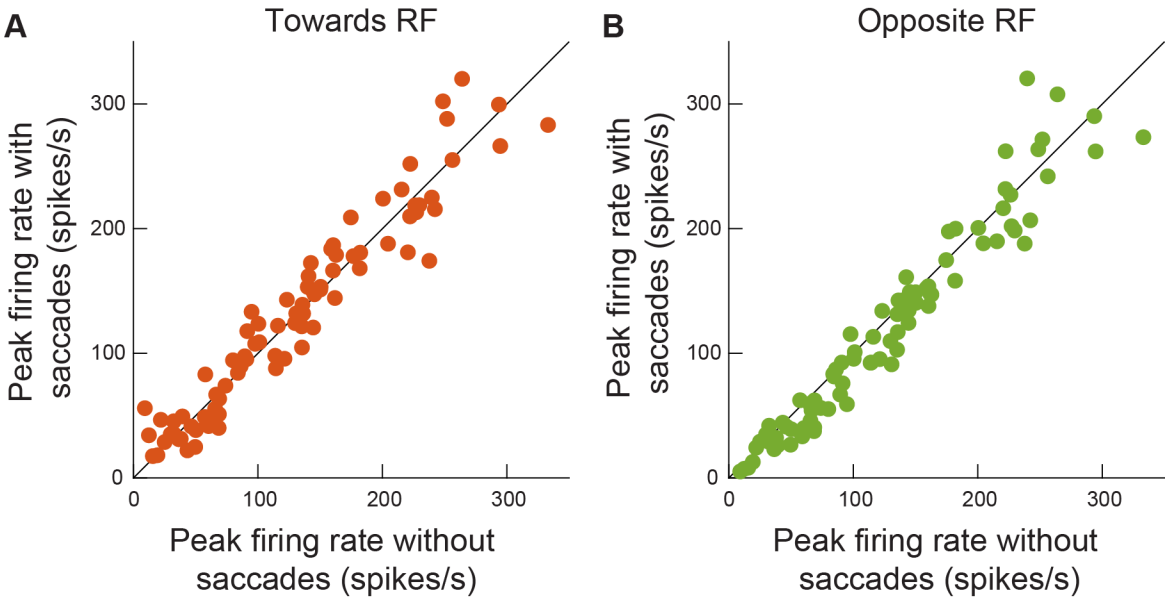

Figure S2 Visual bursts in the SC could happen intra-saccadically whether the movement being generated was towards the recorded neurons' RF locations or opposite them. Peak firing rate for all the recorded neurons when the visual burst was happening with or without microsaccades (similar analyses to Fig. 2, but now separating movement directions relative to RF locations; Methods). **(A)** When microsaccades were going towards the neurons' RF locations (orange), there was no difference between peak firing rate compared to the peak firing rate without microsaccades ($t(84) = -0.3867$, $p = 0.6999$). **(B)** When microsaccades were going opposite to the RF locations (green), the peak firing rate was slightly reduced compared to the peak firing rate without microsaccades ($t(84) = 3.6223$, $p < 4.9876*10^{-4}$), but it was still clearly present. Therefore, regardless of movement directions, intra-saccadic SC visual bursts can still occur.

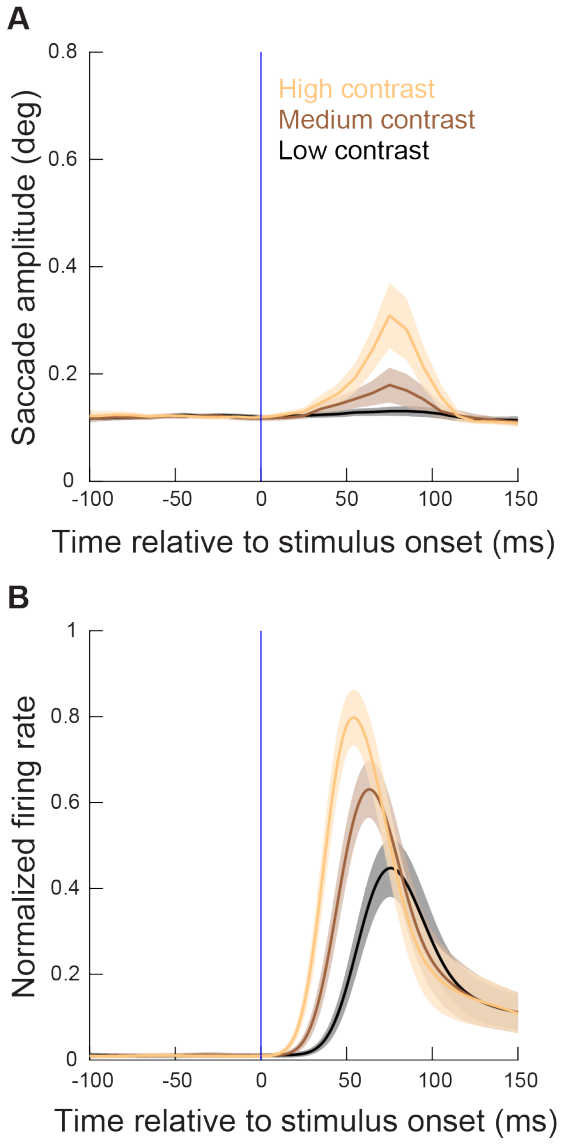

Figure S3 More eccentric stimuli relative to the generated movement amplitudes had weaker effects on metric alterations than the less eccentric stimuli of Fig. 3. (A) Time courses of microsaccade amplitudes relative to stimulus onset when the visual stimuli were presented at eccentricities >4.5 deg (and <20 deg; Fig. 1B). The figure is otherwise formatted identically to Fig. 3. As can be seen, there were weaker effects of more eccentric stimuli on microsaccades, even though the stimuli were made bigger to fill the RF's (Methods) and also even though the raw visual bursts showed similar properties to the more central neurons' visual bursts (**B** and Fig. S4). **(B)** Normalized firing rates of the more eccentric neurons relative to stimulus onset (compared to Fig. 3B). The raw firing rates are shown in Fig. S4, and, together with the current figure, they demonstrate that there was a weaker impact of more eccentric spiking activity on microsaccades; that is, the more eccentric bursts were similar in strength to the more central bursts (Fig. S4), but they still had a smaller impact on microsaccade amplitudes in **A**. Note that, consistent with Hafed and Ignashchenkova (2013); Buonocore et al. (2017b); Malevich et al. (2020a), microsaccade amplitudes at the time of SC visual bursts were decreased relative to baseline (by a small amount) for movements that were opposite the stimulus locations (see Fig. 6). This suggests that visual bursts opposite a planned movement might hamper the movement's execution (Buonocore et al., 2017b).

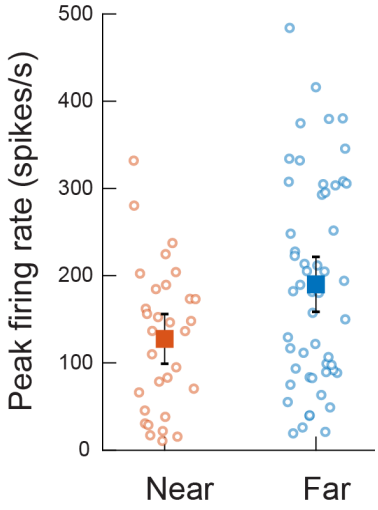

Figure S4 Despite smaller effects on microsaccade amplitudes (Fig. S3), more eccentric visual bursts were not weaker than more central ones. Peak firing rate measurements for neurons with an RF location ≤4.5 deg (Near, orange) or >4.5 deg (Far, blue) from fixation. Each dot represents one neuron. Solid squares represent the averages for each group. Error bars represents two standards error of the mean. In this example, the visual stimuli presented to the neurons were gratings with the second highest contrast.

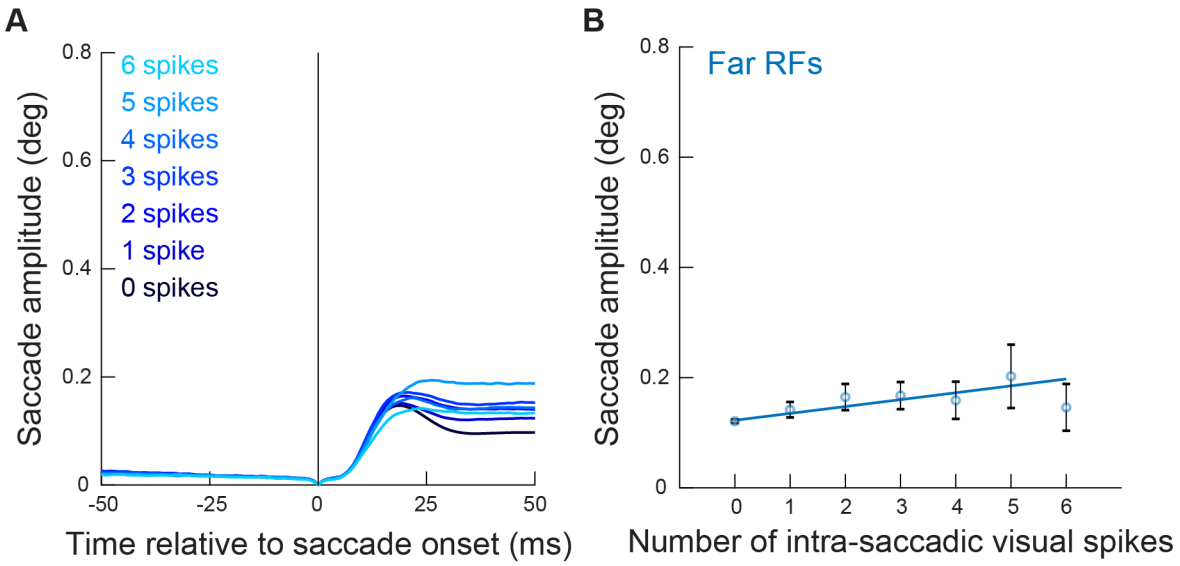

Figure S5 Intra-saccadic "visual" spikes from more eccentric neurons still linearly increased microsaccade amplitudes, but with a much weaker effect size. (A) Radial eye position relative to saccade onset grouped by the number of "visual" spikes counted between movement onset and saccade peak velocity, for eye movements going towards the recorded neuron's RF location (similar to Fig. 4A). In this analysis, the RF was always located at an eccentricity >4.5 deg (Fig. 1B). We used the same grouping and color conventions as in Fig. 4A but in gradients of blue instead of red. When no spikes were recorded during the eye movement, saccade amplitudes were relatively small (darkest blue curve). Adding visual spikes in the SC map during the ongoing movements slightly increased their amplitudes (1 to 6, color-coded from dark to light blue). However, the effect was much milder than for neurons closer in eccentricity to the foveal movement endpoints (Fig. 4A). **(B)** Mean saccade amplitude against the number of intra-saccadic visual spikes (faint blue dots), similar in formatting to Fig. 4B. There was a linear increase in amplitude relative to the number of injected visual spikes (blue line), similar to Fig. 4B for the more central neurons. However, the slop of the effect was significantly lower. The solid lines represent the best linear fit of the underlying raw data. Error bars denote 95% confidence intervals.

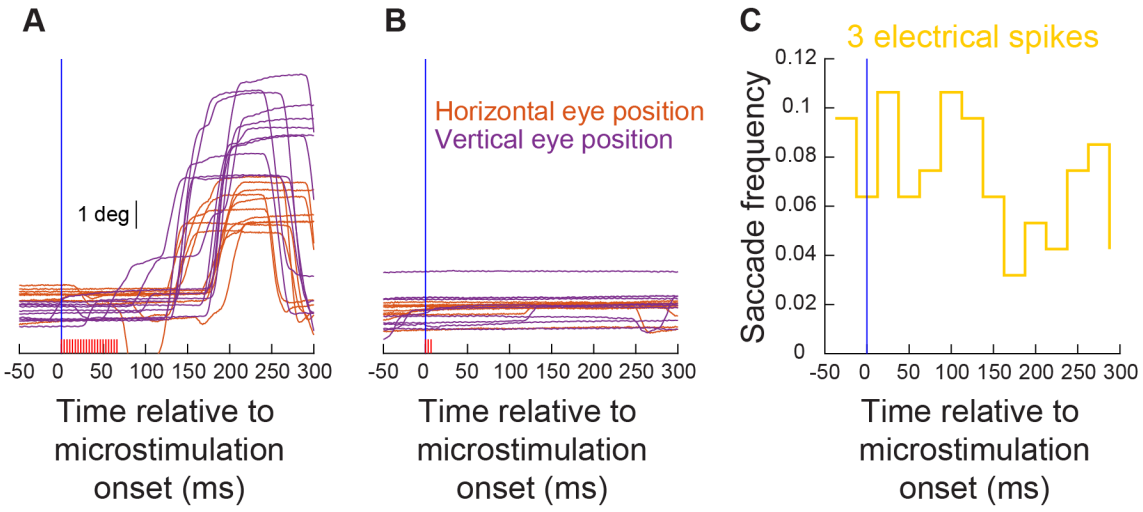

Figure S6 Triple pulse microstimulation, our strongest experimental manipulation in Figs. 6, 7, did not by itself evoke saccades. (A) One example microstimulation session with a short spike train of 70 ms duration at 300Hz and with a current amplitude of 30μA. Horizontal (orange) and vertical (purple) eye positions are shown from individual trials aligned on microstimulation onset (blue line). Soon after the microstimulation pulse train onset, saccadic eye movements were evoked in a direction congruent with the microstimulated SC site (up to the right). About 100 ms later, the eyes made a saccade back to the fixation point to recover, especially since the fixation spot was still visible during the microstimulation train. The red vertical lines on the x-axis indicate each microstimulation pulse with a spacing of 3.3 ms. **(B)** Same as **A**, but with only a train of 3 microstimulation pulses (still at 300Hz and current amplitude of 30μA). No eye movements were systematically evoked after the microstimulation train was applied. The figure shows ten example trials. **(C)** Histogram of saccadic reaction times relative to microstimulation onset during the injection of 3 electrical spikes (the condition in **B**). The frequency of saccades was the same before and after microstimulation, supporting the conclusion that 3 electrical spikes were insufficient, on their own, to evoke eye movements.